Antiferromagnetic Resonance in $MnCl_2 \cdot 4H_2O$ over the Temperature Range 0.32–1.62°K*

M. ABKOWITZ† AND A. HONIG

Department of Physics, Syracuse University, Syracuse, New York

(Received 18 June 1964)

Antiferromagnetic and paramagnetic resonance experiments have been performed on $MnCl_2 \cdot 4H_2O$ ($T_N = 1.62°K$) in the temperature range 1.02 to 4.2°K at 3-cm microwave wavelengths and in the temperature range 0.32 to 4.2°K at 1.2-cm microwave wavelengths. Temperatures below 1°K were achieved with liquid-He³ refrigeration. In the antiferromagnetic state, resonance on the critical-field hyperbola is observed in accordance with the Nagamiya-Yosida theory for orthorhombic anisotropy. The low-field (below critical field) antiferromagnetic resonance behavior, both on and off axis, is also in reasonably good agreement with the theory. Above the critical field, the resonances deviate substantially from the theoretical predictions. This is expected because the Nagamiya-Yosida theory is valid only when the external magnetic field is small compared to the exchange field, and this condition is not satisfied in $MnCl_2 \cdot 4H_2O$ for the high-field resonances. At temperatures below $\sim 0.6°K$, the low-field resonance which occurs with 1.2-cm microwaves and with the external magnetic field parallel to the intermediate anisotropy axis deviates sharply from the theory. Also, below 0.6°K, an additional resonance having some properties similar to critical-field resonance appears at a magnetic-field value lower than the critical field. These low-temperature phenomena may be associated with a modification in the magnetic structure below $\sim 0.6°K$.

I. INTRODUCTION

BELOW 1.62°K, $MnCl_2 \cdot 4H_2O$ is antiferromagnetic as was shown by the magnetization experiments of Henry[1] and the specific-heat experiments of Friedberg and Wasscher.[2] Henry's magnetization measurements lead to a value of 14 000 Oe for the molecular field at 0°K, and Gijsman et al.[3] estimate from radio-frequency measurements that the 0°K critical field for spin flop-over is 7500 Oe. Combining these results, the anisotropy in the molecular field is estimated to be about 15% at 0°K, which is relatively large compared to the extensively studied orthorhombic antiferromagnet $CuCl_2 \cdot 2H_2O$.[4] The strength of the internal molecular field in $MnCl_2 \cdot 4H_2O$ is comparable to that of readily accessible laboratory fields. This gives rise to interesting effects at high external magnetic fields, such as sizable shifts in the Néel temperature produced by a magnetic field directed along the preferred c axis,[3] and the quadratic field dependence of the antiferromagnetic parallel susceptibility.[5]

The presently available temperature-dependent theories of antiferromagnetic resonance are subject to the restriction that the internal field be much greater than the external field. It seemed of interest to investigate the antiferromagnetic resonance of $MnCl_2 \cdot 4H_2O$, since existing theory is applicable and can be tested over part of the external-field range, whereas new phenomena might be expected to occur at high external fields

where no theory is yet appropriate. The temperature dependence of the relatively large anisotropy could also be expected to shed light on the applicability of the molecular-field model. Earlier antiferromagnetic resonance work on $MnCl_2 \cdot 4H_2O$ at microwave frequencies[6] was severely limited because the experimental temperatures accessible were not sufficiently below the Néel temperature. The construction of a liquid-helium-3 cooled, 1.2-cm-band (~ 24 Gc/sec) magnetic-resonance spectrometer[7] permitted us in the present study to measure resonances down to 0.32°K at ~ 24 Gc/sec. These studies were supplemented by 3-cm-band (~ 9.2 Gc/sec) microwave measurements down to 1.025°K.

II. EXPERIMENTAL CONSIDERATIONS

1. Samples

There are two crystallographic forms of $MnCl_2 \cdot 4H_2O$. The β phase originally studied by Dawson and Williams[8] grows from a saturated solution in the temperature range 0–6°C and is believed to be isomorphous with $FeCl_2 \cdot 4H_2O$.[9] The form of $MnCl_2 \cdot 4H_2O$ used in our experiments is grown at room temperature and is referred to as the α phase. A complete x-ray study of α-$MnCl_2 \cdot 4H_2O$ which yields the positional parameters of the atoms in the unit cell has recently been reported by Zalkin et al.[9] They find that the crystal belongs to the monoclinic system and has a primitive unit cell containing four formula units. The angle β is 99.74 $\pm 0.04°$, and thus the deviation from the orthorhombic system is not large. The structure consists of discrete

* Research supported by a grant from the National Science Foundation.
† Present address: Department of Physics, University of Pittsburgh, Pittsburgh, Pennsylvania.
[1] W. E. Henry, Phys. Rev. **91**, 431 (1953).
[2] S. A. Friedberg and J. D. Wasscher, Physica **19**, 1072 (1953).
[3] H. M. Gijsman, N. J. Poulis, and J. Van Den Handel, Physica **25**, 954 (1959).
[4] J. Ubbink, thesis, Leiden, 1953 (unpublished); H. J. Gerritsen, thesis, Leiden, 1955 (unpublished).
[5] M. A. Lasheen, J. Van Den Brock, and C. J. Gorter, Physica **24**, 1061 (1958).

[6] B. Bolger, Proceedings of the Conference on Low Temperature Physics, Paris, 1955, p. 244 (unpublished).
[7] M. Abkowitz and A. Honig, Rev. Sci. Instr. **33**, 568 (1962).
[8] H. M. Dawson and P. Williams, Z. Physik Chem. **31**, 59 (1899).
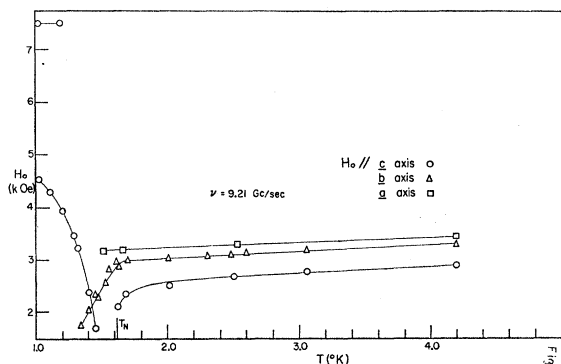[9] A. Zalkin, J. D. Forrester, and D. H. Templeton, Inorg. Chem. **3**, 529 (1964).

FIG. 1. Resonant magnetic field for H_0 parallel to the crystal axes versus temperature for $MnCl_2 \cdot 4H_2O$ at $\nu = 9.21$ Gc/sec. c, b, and a are magnetically most preferred, intermediate, and least preferred axes. Antiferromagnetic and paramagnetic regions are shown.

slightly distorted octahedral groups with each manganese atom coordinated to two chlorine atoms at an average distance of 2.488 Å and to four oxygen atoms at an average distance of 2.206 Å. The chlorine atoms are adjacent in each octahedron, rather than opposite as in the $FeCl_2 \cdot 4H_2O$ structure. Unfortunately, no neutron diffraction work has come to our attention, and thus the magnetic space group is unknown.

The α-phase $MnCl_2 \cdot 4H_2O$ crystals are grown by evaporation at room temperature from the saturated solution. The crystals generally develop as flat, pink, optically clear plates with the (100) face prominent. These single crystals are fairly unstable when removed from solution and readily give up their water of hydration, leaving an opaque pink powder residue. They can be preserved, however, by storing in oil, and the oil can be subsequently removed by immersing the sample in carbon tetrachloride. Decomposition of the crystals is enhanced in vacuum, and since it was necessary for the crystal to remain under vacuum for several hours when employing the He^3 cryostat, a safe method of encapsulation was required which would not interfere with good thermal contact. A thin pressure-setting adhesive teflon tape served the purpose adequately. Sample weights varied from about 1 to 100 mg.
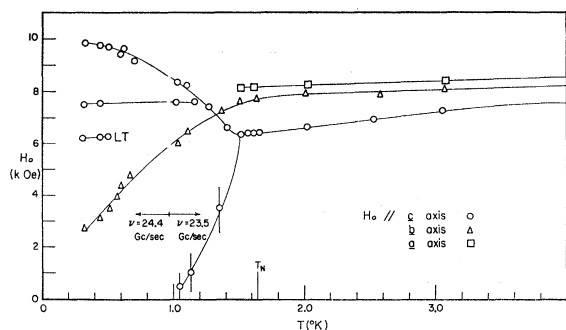

FIG. 2. Resonant magnetic field for H_0 parallel to the crystal axes versus temperature for $MnCl_2 \cdot 4H_2O$. $\nu = 24.4$ Gc/sec for $T < 1.02°K$ and $\nu = 23.5$ Gc/sec for $T \geq 1.02°K$. Antiferromagnetic and paramagnetic regions are shown.

2. Cryogenics and Microwave Apparatus

Experiments were performed with 3-cm-band (~ 9.2 Gc/sec) and 1.2-cm-band (~ 24 Gc/sec) microwaves. The resonant cavities were of the reflection type, operating in the TE_{102} mode. 9.2-Gc/sec measurements were made in the liquid-helium-4 temperature range of 1.02 to 4.2°K. It was possible to rotate the crystal with respect to the cavity with this system. The measurements at 24 Gc/sec were performed between 0.32 and 4.2°K. The region between 0.32 and 1.02°K was made accessible by means of liquid-helium-3 refrigeration.[7] Biased crystal detection was employed for adequate signal at fractional-microwatt power levels.

Two methods were used to display the detector output. In the first method, which was utilized for determining line shapes, the microwave oscillator was frequency-stabilized and adjusted in frequency at each point on the resonance to correct for the cavity detuning caused by the dispersion. The absorption line shape was then obtained from a point-by-point plot of the crystal output, as measured on a microammeter. In the second method, the microwave oscillator was swept over about 50 Mc/sec and the cavity-plus-sample absorption was displayed on an oscilloscope. As the magnetic field was swept through resonance, the position on the oscilloscope face of minimum reflected power shifted in both the horizontal and vertical directions, corresponding to dispersion and absorption. The magnetic-field value for maximum absorption coincides with that of zero dispersion, and thus the maximum of the absorption can be obtained visually. This method proved to be as accurate as the line-shape plot for the purpose of locating the center of the resonance and was less time-consuming. Linewidth determinations are subject to substantial error because of the very strong microwave absorption present for even our smallest usable samples. Compensating corrections were not made in this study, since our main interest was in the position of the resonance maxima. Qualitative reference to linewidth data subject to errors which can be as large as 30% are nevertheless noted.

Considerable care had to be exercised to prevent microwave heating effects, particularly in the 24-Gc/sec microwave experiments. Even when the sample was immersed in superfluid liquid helium, the incident power had to be kept below 1 μW. This is strikingly illustrated by the shift from 6800 to 5980 Oe of the 24-Gc/sec b-axis resonance at 1.025°K (see Fig. 2) when the incident power was reduced from 10 to 1 μW. Microwave heating effects were not pronounced in the 9.2-Gc/sec experiments for power levels below 100 μW.

III. EXPERIMENTAL RESULTS

1. Paramagnetic State and Transition Region

The crystallographic axes c, b, and a are, respectively, the most favored, next most favored, and least favored

directions of the magnetization in MnCl$_2$·4H$_2$O. The g factor and linewidth are isotropic between liquid-nitrogen temperature and room temperature. The g factor is 2.00 and the linewidth varied from about 600 Oe at room temperature to about 1600 Oe at 77°K. In the liquid-helium region, both the linewidth and g factor become anisotropic. The linewidth anisotropy at 4.2°K was demonstrated by Bolger,[6] and our observations concur with his, yielding a linewidth of about 2200 Oe when the external magnetic field H_0 is parallel to the c axis, and a linewidth of about 1700 Oe when H_0 is along the other axes. As the temperature is lowered from 4.2°K to the Néel temperature of 1.62°K, the lines become weaker and broader. The apparent g-factor anisotropy is implicit in Figs. 1 and 2, where resonant external magnetic field is plotted against temperature at two different microwave frequencies, and is directly shown in Fig. 3.

In the transition region near the Néel temperature T_N, several features that are not obvious from Figs. 1 and 2 are worth noting. The a-axis resonances (H_0 parallel to the a axis) persist slightly below T_N, disappearing below 1.5°K at both 9.2 and 24 Gc/sec. The b-axis resonances at 9.2 and 24 Gc/sec are continuous between the paramagnetic and antiferromagnetic regions. The 9.2-Gc/sec c-axis resonance disappears at the Néel temperature (see Fig. 1), and as the temperature is lowered, the antiferromagnetic resonance first becomes observable at 1.45°K. At 24 Gc/sec, the c-axis paramagnetic and antiferromagnetic resonances join smoothly, as is seen in Fig. 2.

2. Antiferromagnetic State

For the axial resonance data (H_0 parallel to c, b, and a axes), we again refer to Figs. 1 and 2. The c-axis critical-field resonance absorption at 7500 Oe is seen both at 9.2 and 24 Gc/sec in Figs. 1 and 2, respectively. This resonance, which corresponds to spin flopping, is temperature-independent and is observed only below 1.18°K. In what follows, the resonances will be classified as low-field resonances if they occur at magnetic fields smaller than the critical field and as high-field resonances if they occur at magnetic fields larger than the critical field. Low-field resonances at 9.2 Gc/sec are seen in Fig. 1 along the c, b, and a axes. The b-axis resonance disappears below 1.35°K and no a-axis resonance is seen below 1.5°K. High-field resonances were not observed at 9.2 Gc/sec. In Fig. 2, in addition to the critical-field resonance at 7500 Oe already mentioned, three other c-axis resonances are found. One is a high-field resonance. A second appears only below 0.60°K at about 6100 Oe and is about one-fourth the amplitude of the critical-field resonance. It is given a special name, LT (for low temperature), since it does not seem to be related to the theory. The third terminates at zero field at about 1.0°K. This latter resonance does not exhibit well-defined peaks since the absorption
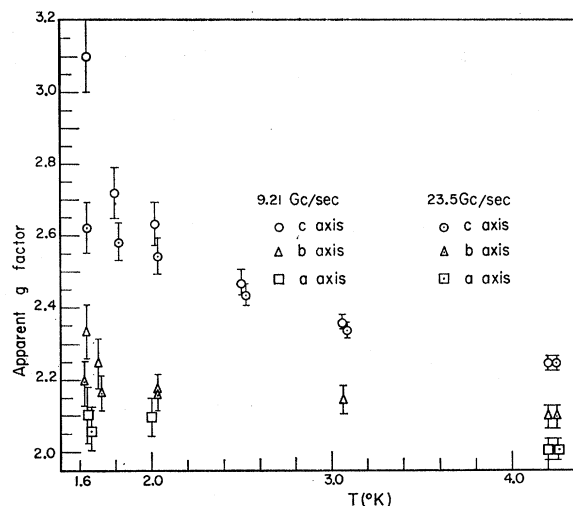

FIG. 3. Paramagnetic-resonance apparent g values versus temperature between 4.2 and 1.62°K for the external magnetic field along the c, b, and a axes.

extends very asymmetrically to zero field. The vertical lines associated with the points on Fig. 2 for this low-field resonance give the external-field range corresponding to steepest slope of the absorption edge.

All the resonances with the exception of the critical-field resonance and the LT resonance have maximum amplitude when the microwave field H_{rf} is perpendicular to the external magnetic field H_0. The critical-field resonance has maximum amplitude when H_{rf} makes a small angle with H_0. This angle is frequency-dependent and is about 20° at 9.2 Gc/sec for H_0 along the c axis. These polarization effects are similar to those
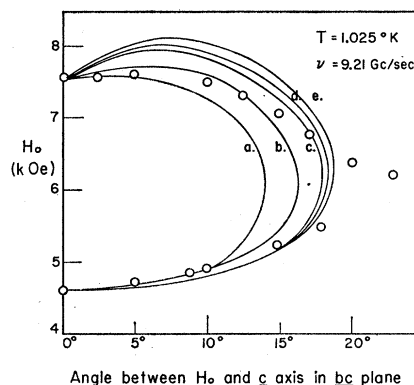

Angle between H$_0$ and c axis in bc plane

FIG. 4. Antiferromagnetic-resonant field versus angle between H_0 and the c axis in the bc plane of MnCl$_2$·4H$_2$O. T=1.025°K, ν=9.21 Gc/sec. Solid curves give the theoretical resonance values expected from the Nagamiya-Yosida theory. The different curves a, b, c, d, and e correspond to the following choices of the three parameters α, $2K_1/\chi_\perp$ ($\equiv C_1$), $2K_2/\chi_\perp$ ($\equiv C_2$):

	α	$C_1 \times 10^{-6}$ Oe^2	$C_2 \times 10^{-6}$ Oe^2
a.	0.495	27.8	87.7
b.	0.580	32.6	77.6
c.	0.640	36.0	70.5
d.	0.660	37.1	70.0
e.	0.685	38.5	69.0

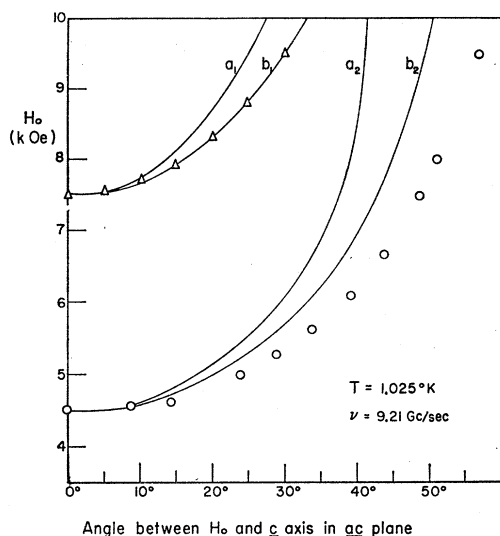Angle between H_0 and $\underline{c}$ axis in $\underline{ac}$ plane

Fig. 5. Antiferromagnetic-resonant field versus angle between H_0 and the c axis in the ac plane. $T=1.025°\mathrm{K}$, $\nu=9.21$ Gc/sec. Solid curves give the theoretical resonance values expected from the Nagamiya-Yosida theory. Curves a_1, a_2, b_1, b_2 correspond to the following choice of the three parameters α, $2K_1/\chi_\perp$ ($\equiv C_1$), $2K_2/\chi_\perp$ ($\equiv C_2$):

	α	$C_1 \times 10^{-6}$ Oe^2	$C_2 \times 10^{-6}$ Oe^2	
a_1	0.660	37.1	70.0	(Critical-field resonance)
a_2	0.660	37.1	70.0	(Low-field resonance)
b_1	0.495	27.8	87.7	(Critical-field resonance)
b_2	0.495	27.8	87.7	(Low-field resonance)

reported in studies[10] of $CuCl_2 \cdot 2H_2O$. The polarization dependence of the LT resonance was not accurately determined, but it was somewhere in between that of the critical-field and paramagnetic-like resonances.

In Figs. 4 through 10, resonance data are presented for H_0 in the bc and in the ac planes. Theoretical curves based on the Nagamiya-Yosida theory are included in some of the figures, but discussion of these is postponed until the next section. Figures 4 and 5 summarize the 9.2-Gc/sec resonance data for H_0 in the bc and ac planes, respectively, and in the neighborhood of the c axis in both. The upper curve of Fig. 5 (ac plane) is the critical hyperbola. The direction of H_{rf} was adjusted for separately optimizing the low-field and critical-field resonances. Resonances are not found at 9.2 Gc/sec in the neighborhood of the b or a axes at $1.025°\mathrm{K}$. Figures 6 and 7 present the 24-Gc/sec resonance data for H_0 in the bc plane in the neighborhood of the c axis, at two different temperatures. It is noted that the resonance branch which terminates in the critical-field resonance at 7500 Oe when H_0 is parallel to the c axis ($0°$ angle) is measurable only within about $5°$ of the c axis. This is quite distinct from the behavior in the bc plane at 9.2 Gc/sec (see Fig. 4). The high-field resonance is shown in conjunction with its decreasing amplitude as H_0 is rotated from the c axis. In Fig. 6, corresponding to $T=1.025°\mathrm{K}$, the critical-field and the high-field
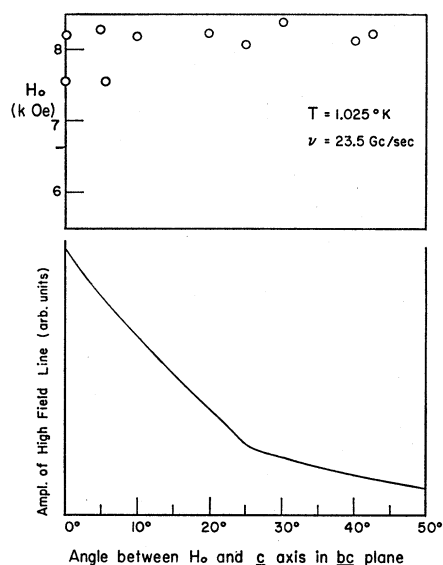
[10] H. J. Gerritsen and M. Garber, Physica **22**, 197 (1956).

Angle between H_0 and $\underline{c}$ axis in $\underline{bc}$ plane

Fig. 6. Antiferromagnetic-resonant field versus angle between H_0 and the c axis in the bc plane of $MnCl_2 \cdot 4H_2O$. $T=1.025°\mathrm{K}$, $\nu=23.5$Gc/sec. Amplitude of high-field resonance versus angle is shown in the lower part of the figure.

resonances are resolved by virtue of their different dependences on direction of the microwave field H_{rf}. In Fig. 7, however, where the temperature is $0.44°\mathrm{K}$, the high-field resonance is easily resolved from the
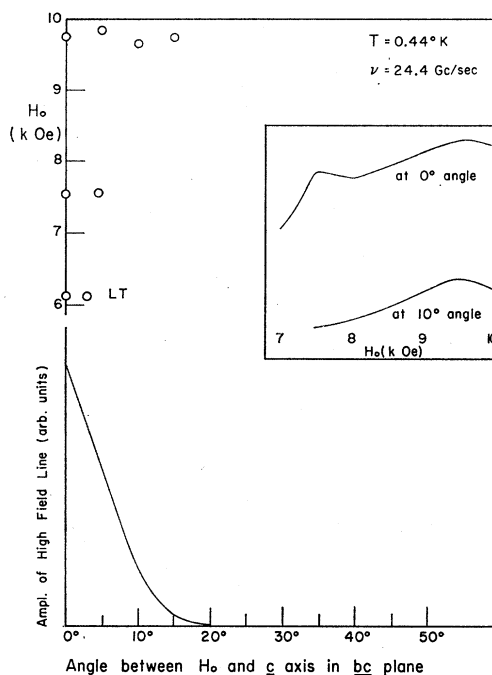

Angle between H_0 and $\underline{c}$ axis in $\underline{bc}$ plane

Fig. 7. Antiferromagnetic-resonant field versus angle between H_0 and c axis in bc plane of $MnCl_2 \cdot 4H_2O$. $T=0.44°\mathrm{K}$, $\nu=24.4$ Gc/sec. LT is an additional resonance which appears only at low temperature. Amplitude of high-field resonance versus angle is shown in lower part of figure. Absorption line shapes are given in insert.
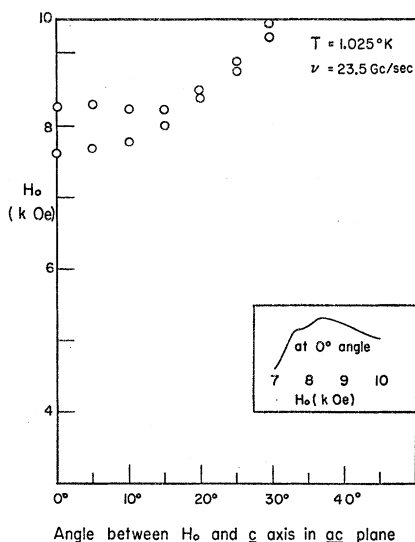
FIG. 8. Antiferromagnetic-resonant field versus angle between H_0 and the c axis in the ac plane of $MnCl_2 \cdot 4H_2O$. $T = 1.025°K$, $\nu = 23.5$ Ge/sec. Absorption line shape is given in insert. Lines are resolved at larger angles by virtue of different microwave-field polarization dependence.

critical-field resonance, as is shown in the insert for H_0 along the c axis (0° angle). The direction of H_{rf} was adjusted here so that both lines were simultaneously observable. For H_0 rotated 10° from the c axis, the branch which terminates on the c-axis critical-field resonance is no longer observable, and thus the high-field resonance appears alone, as is seen in the insert of Fig. 7. The LT resonance appears in Fig. 7 at 6100 Oe, and it is measurable for only about a 3° rotation in the plane. Figures 8 and 9 show the 24-Gc/sec data for H_0 in the ac plane and in the neighborhood of the c axis. The critical-field resonance starting at 7500 Oe when H_0 is parallel to the c axis persists well into the ac plane, generating the same critical hyperbola as
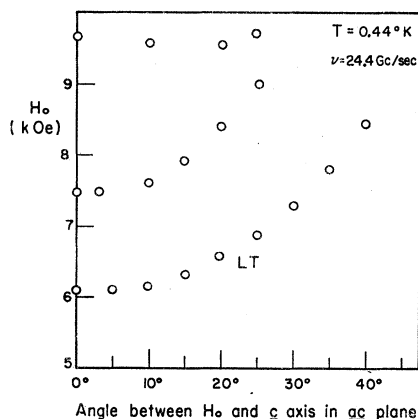

FIG. 9. Antiferromagnetic-resonant field versus angle between H_0 and the c axis in the ac plane of $MnCl_2 \cdot 4H_2O$. $T = 0.44°K$, $\nu = 24.4$ Gc/sec. LT is additional resonance which appears only at low temperature.

at 9.2 Gc/sec (see Fig. 4). In Fig. 8, the insert indicates the barely resolved critical- and high-field resonances when the direction of H_{rf} is such as to permit both lines to be simultaneously seen. Proper selection of the direction of H_{rf} allowed the lines to be clearly resolved. At a temperature of 0.44°K, the resonances become well separated, as seen in Fig. 9. The falloff in amplitude as H_0 rotates into the ac plane is not shown but is similar to the bc-plane results seen in Figs. 6 and 7, with an indication of the rapidity of amplitude falloff provided by the extent of angle for which measurements were taken. Figure 9 also gives the angular dependence in the ac plane of the LT resonance. It is quite similar to that of the critical-field hyperbola. In Fig. 10, the resonances are plotted at three different temperatures for 24-Gc/sec frequency and H_0 in the bc plane but in the neighborhood of the b axis.

The linewidths of most of the antiferromagnetic resonances were about 1600 Oe. The exceptions were the widths of the critical-field resonance and the LT resonance. These latter resonances had linewidths of about 800 Oe. Hysteresis in the critical-field resonance was observed to a varying degree from sample to sample, with the resonance field shifting as much as 500 Oe depending on the direction of field sweep for one sample. Samples with much smaller hysteresis (less than 100 Oe) were used for determining the critical-field values, and the average resonance field for both sweep directions was used.
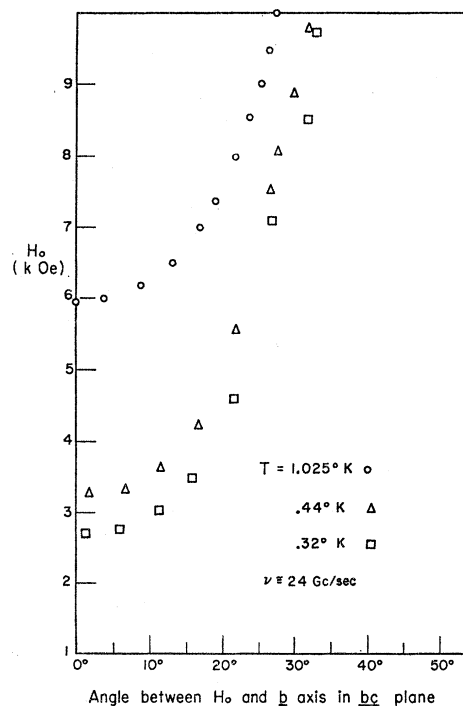

FIG. 10. Antiferromagnetic resonant field versus angle between H_0 and b axis in bc plane of $MnCl_2 \cdot 4H_2O$. $T = 1.025$, 0.44, and 0.32°K. $\nu = 24.4$ Gc/sec at 0.44 and 0.32°K, and $\nu = 23.5$ Gc/sec at 1.025°K.
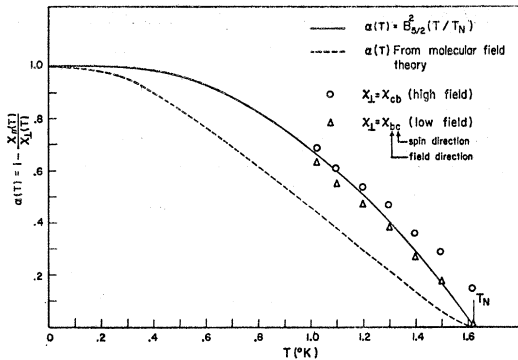
FIG. 11. Temperature dependence of $\alpha(T) \equiv 1 - \chi_{\parallel}(T)/\chi_{\perp}(T)$. Solid curve represents $\alpha(T) = B_{5/2}{}^2(T/T_N)$, which is deduced from phenomenological arguments. Experimental points between 1.02 and 1.62°K are obtained from the magnetization data of Gijsman et al. ($\chi_{\parallel}$ is taken from the low-field magnetization data and $\chi_{\perp}$ from both low- and high-field magnetization data.) Dashed curve is computed from molecular-field theory (see Ref. 11).

IV. COMPARISON WITH THE THEORY OF NAGAMIYA AND YOSIDA FOR AN ORTHORHOMBIC ANTIFERROMAGNET

Nagamiya and Yosida[11] have worked out the theory of two-sublattice antiferromagnetic resonance for orthorhombic anisotropy subject to the restrictions that the anisotropy energy and Zeeman energy are small compared with the exchange energy. These conditions hold approximately for our low-field results. In order to compare experimental results with the theory at all temperatures, it is necessary to know $(1 - \chi_{\parallel}(T)/\chi_{\perp}(T))$, which is called $\alpha(T)$. $\chi_{\parallel}(T)$ and $\chi_{\perp}(T)$ are, respectively, the parallel and perpendicular magnetic susceptibilities. In previous analyses of antiferromagnetic resonance, it was found that a better fit of the resonance data is obtained if the experimental susceptibilities are inserted in the Nagamiya-Yosida resonance expressions rather than using the susceptibilities calculated from the molecular-field theory itself.[12] This is indeed a phenomenological procedure, but one which has been justified recently by Kanamori and Tachiki[13,14] who derived the same antiferromagnetic resonance equations in terms of phenomenological susceptibilities and anisotropy constants without resort to molecular fields. In the case of $MnCl_2 \cdot 4H_2O$, susceptibility measurements in the antiferromagnetic state[3] have been made down to 1.02°K. Our experiments range down to 0.32°K, and thus a variant procedure, which is described below, was used to obtain the phenomenological function $\alpha(T)$ over the entire temperature range of interest.

In the Nagamiya-Yosida theory, the anisotropy constants K_1 and K_2 are introduced via the orthorhombic

[11] T. Nagamiya, K. Yosida, and R. Kubo, Advan. Phys. 4, 2 (1955).
[12] S. Foner, *Magnetism 1* (Academic Press Inc., New York, 1963).
[13] J. Kanamori and M. Tachiki, J. Phys. Soc. Japan 17, 1384 (1962).
[14] J. Kanamori and M. Tachiki, J. Phys. Soc. Japan 17, 64, Suppl. B-1 (1962).

anisotropy energy density which is written as

$$E_A = \tfrac{1}{2}K_1(\beta_+{}^2 + \beta_-{}^2) + \tfrac{1}{2}K_2(\gamma_+{}^2 + \gamma_-{}^2). \qquad (1)$$

α_+, β_+, γ_+, and α_-, β_-, γ_- are the direction cosines of the plus and minus sublattice magnetization vectors with the c, b, and a axes, respectively. The theory gives the expression for the critical field, H_C, when H_0 is parallel to the preferred c axis.

$$H_C = [2K_1/(\chi_{\perp} - \chi_{\parallel})]^{1/2}. \qquad (2)$$

Using the definition of $\alpha(T)$ in terms of the susceptibilities, one obtains from Eq. (2)

$$\alpha(T) = 2K_1(T)/H_C{}^2(T)\chi_{\perp}(T). \qquad (3)$$

Since H_C was found experimentally to be temperature-independent throughout the temperature range studied (see Figs. 1 and 2), and since $\chi_{\perp}$ exhibits only a very slight temperature dependence[3] between 1.02 and 1.62°K, we assign to $\alpha(T)$ the same temperature dependence as $K_1(T)$. Thus

$$\alpha(T)/\alpha(0) = K_1(T)/K_1(0). \qquad (4)$$

An assumption frequently made in molecular-field theory is that the temperature dependence of the sublattice magnetization is that of a reduced Brillouin function. This assumption has been found in several materials[15] to be experimentally valid to a reasonable degree (in contrast to the molecular-field determination of the susceptibilities), and results in the expression

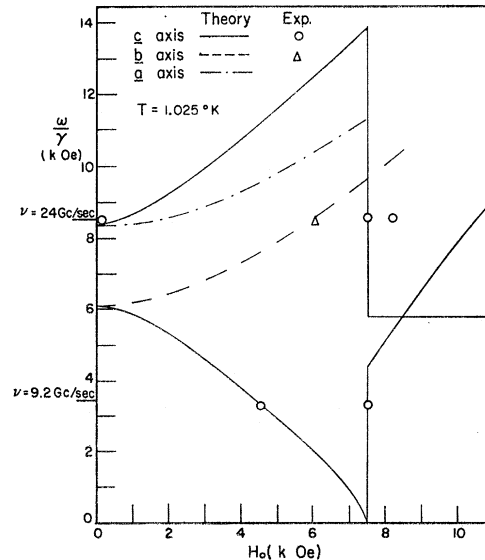$$K_1(T)/K_1(0) = K_2(T)/K_2(0) = B_S{}^2(T/T_N), \qquad (5)$$

FIG. 12. Antiferromagnetic "frequency"-field diagram calculated from Nagamiya-Yosida theory for H_0 parallel to c, b, and a axes at $T = 1.025$°K. Experimental points are also shown.

[15] See for example S. M. Johnson and A. H. Nedercot, Phys. Rev. 114, 705 (1959); and J. J. Stickler and G. S. Heller, J. Appl. Phys. Suppl. 33, 1302 (1962).
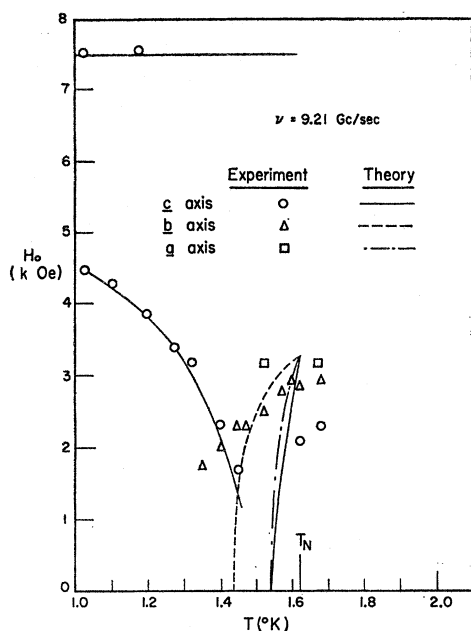
FIG. 13. Axial antiferromagnetic resonances in MnCl₂·4H₂O versus temperature compared to predictions of Nagamiya-Yosida theory. $\nu = 9.21$ Gc/sec.

where $B_S(T/T_N)$ is the reduced Brillouin function for spin S. Combining Eqs. (4) and (5), and including the fact that $\alpha(0) = 1$, we get

$$\alpha(T) = B_S^2(T/T_N). \tag{6}$$

Using the value $S = \frac{5}{2}$ appropriate for MnCl₂·4H₂O in Eq. (6) yields an $\alpha(T)$ curve which is a good approximation to the experimental $\alpha(T)$ values computed from the magnetization data of Gijsman et al.[3] This agreement is displayed in Fig. 11; it supports our use of Eq. (5) for MnCl₂·4H₂O. The poor fit to the experimental points, of $\alpha(T)$ derived from the molecular-field-determined susceptibilities, is also shown in Fig. 11, and is in accord with observations on other related materials.[16]

In addition to $\alpha(T)$, two parameters C_1 $(\equiv 2K_1/\chi_\perp)$ and C_2 $(\equiv 2K_2/\chi_\perp)$ are needed in order to make the theory completely determined, and thence applicable to our results at all temperatures, microwave frequencies, and directions of H_0. The data chosen to fix the anisotropy parameters are the 9.2-Gc/sec c-axis resonances at 1.025°K. The resonance at 7500 Oe has already been referred to as the critical-field resonance and was identified as such from its approximate agreement with the critical-field resonance value reported by Gijsman et al.,[3] its unique amplitude dependence on direction of the microwave field, its existence at the same external magnetic field at both 9.2 and 24 Gc/sec, and its characteristic critical-field hyperbola seen in Figs. 5, 8, and 9. One notes that this critical-field

[16] J. Ubbink, thesis, Leiden, 1953 (unpublished).

resonance is measurable only below 1.18°K. Although this is considerably below the zero-field Néel temperature of 1.62°K, it is only 0.10° below the 1.28°K modified Néel temperature due to a 7500-Oe external magnetic field along the c axis.[3] (We neglect in the following calculations the shifts in T_N produced by the external field. It is not clear how to incorporate this effect in the resonance theory, and the shifts are relatively small at fields below 4500 Oe along the c axis and below 10 000 Oe along the b axis, where most of our resonances which are amenable to interpretation within the framework of the theory occur.) Substituting the values of H_C and $\alpha(1.025)$ in Eq. (3) gives

$$C_1(1.025) = 37.1 \times 10^6 \text{ Oe}^2. \tag{7}$$

The Nagamiya-Yosida theory gives the following resonance equation for H_0 parallel to the preferred c axis and less than the critical field:

$$(\omega/\gamma)^2 = \frac{1}{2}\{H^2(1+\alpha^2) + C_2 + C_1 \pm [H^4(1-\alpha^2)^2 + 2H^2(1+\alpha)^2(C_2+C_1) + (C_2-C_1)^2]^{1/2}\}. \tag{8}$$

We identify this resonance with the observed low-field line at 4500 Oe (see Fig. 1), and obtain from Eq. (8)

$$C_2(1.025) = 70.0 \times 10^6 \text{ Oe}^2. \tag{9}$$

The "frequency"-field diagrams for H_0 parallel to the crystal axes can now be computed at all temperatures from the theory. The equations by which this is done are Eq. (8) and

$$(\omega/\gamma)^2 = H^2 - C_1, \quad \text{when} \quad H_0 > H_C, \; H_0 \| c, \tag{10a}$$

$$(\omega/\gamma)^2 = H^2 + C_1, \quad \text{when} \quad H_0 \| b, \tag{10b}$$

$$(\omega/\gamma)^2 = H^2 + C_2, \quad \text{when} \quad H_0 \| a. \tag{10c}$$

The temperature-dependent values of α, C_1, and C_2 are obtained from Eqs. (5), (6), (7), and (9). In Fig. 12, the diagram at $T = 1.025$°K is shown, as well as points corresponding to observed resonances. The two
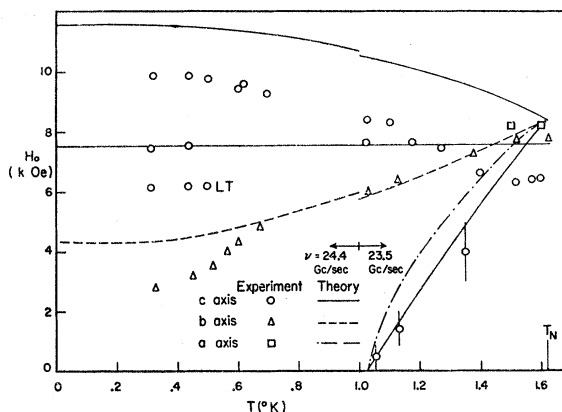

FIG. 14. Axial antiferromagnetic resonances in MnCl₂·4H₂O versus temperature compared to predictions of Nagamiya-Yosida theory. $\nu \approx 24$ Gc/sec.

points at 9.2 Gc/sec are of course those used to compute the parameters from which the theoretical curves were drawn. At 24 Gc/sec, however, it is seen that the diagram predicts a critical-field resonance at the same field as for 9.2 Gc/sec, which was observed, as well as four other resonances, three at low field and one at high field. Of the three predicted low-field resonances, two are seen to agree well with the theory, and the third is absent. The absent resonance is along the a axis, which is the monoclinic axis in $MnCl_2 \cdot 4H_2O$ and therefore the axis least expected to correspond to the orthorhombic theory. The discrepancy of the high-field resonance is not surprising, since the theory breaks down for external fields comparable to the exchange field.

The theoretical curves in Figs. 13 and 14 are computed from the axial resonance equations, Eqs. (8) and (10), at each temperature. The 9.2-Gc/sec comparison of experiment and theory in Fig. 13 shows excellent agreement along the c axis. It is noted that the theory includes a cutoff in the resonance at 1.45°K, as is observed. The correspondence along the b axis is qualitatively satisfactory. Again, the a-axis data bear no resemblance to the theory, which is partly attributed to a being the monoclinic axis of the crystal. In Fig. 14, which illustrates a comparison of axial resonance theory and experiment at 24 Gc/sec, the critical resonance over the whole temperature range and the b-axis resonance down to about 0.7°K fit the theory very well. Below 0.6°K, the b-axis resonance deviates markedly from the theory and a new c-axis resonance, denoted by LT, appears. Neither of these phenomena is understandable within the context of the unmodified theory, especially since they take place at relatively low fields where the theory should be applicable. The a-axis predicted resonances again are not found, and the high-field resonances are considerably displaced from the theoretical predicted values.

The resonance equations when H_0 lies in the bc plane, and the resonance equations when H_0 lies in the ac plane and is less than the critical field, are complicated and must be solved by an iterative procedure. These equations were programmed for a computer and solved at 9.2 Gc/sec. The solutions provided the basis of a variation-of-parameters study with respect to α, C_1, and C_2. The results of this study are seen in Figs. 4 and 5. In Fig. 4, although none of the sets of parameters can be made to fit all the experimental points, they all lead to a qualitative fit. Curve d, which corresponds to the actual parameters used in fitting the axial data, is reasonably satisfactory for the off-axis data also. In Fig. 5, the ac-plane curves a_1 and a_2 generated from the parameters chosen to fit the axial data deviate substantially from the experimental points. If a fit of the critical-field hyperbola is forced by a change in parameters, curves b_1 and b_2 result. The ac-plane agreement is improved, but the bc-plane agreement is worsened, as seen from curve a of Fig. 4.

Solution of the off-axis resonance equations at 24 Gc/sec was not carried out.

To summarize this section, we can say that the resonance equations of Nagamiya and Yosida describe the 9.2-Gc/sec experimental antiferromagnetic resonances reasonably well both on and off axis, with the exception of a-axis resonance. At 24 Gc/sec, substantial agreement with the theory exists except along the a axis, at high fields and at very low temperature $(T < 0.6°K)$.

V. DISCUSSION

1. Paramagnetic State

Bolger[6] attributed the large anisotropic linewidth in $MnCl_2 \cdot 4H_2O$ at 4.2°K to dipole-dipole interactions but did not elaborate on the corresponding g factors. The temperature dependence of the anisotropic g factors between 4.2°K and $T_N(1.62°K)$, as well as the frequency-dependent g shifts between 2.0 and 1.62°K (see Fig. 3), strongly suggest the importance of short-range order and local microscopic-field effects in addition to the usual demagnetization-field effects. Demagnetization-field corrections computed from susceptibility data lead one to expect apparent g shifts of the order of those observed along the a axis. These can account for only about 15% of the observed g shifts along the c axis.

2. Antiferromagnetic State

Among the orthorhombic and monoclinic materials whose Néel temperature lies in the liquid-helium temperature range, $CuCl_2 \cdot 2H_2O$[4] and $CoCl_2 \cdot 6H_2O$[17] have been extensively investigated in the microwave region prior to present work on $MnCl_2 \cdot 4H_2O$. Despite the considerable differences in anisotropy and exchange energies among these antiferromagnets, they exhibit very similar qualitative features in their microwave-frequency antiferromagnetic resonance behavior. The Nagamiya-Yosida theory for a two-sublattice orthorhombic crystal in which the exchange energy is much greater than the Zeeman and anisotropy energies is well suited to $CuCl_2 \cdot 2H_2O$, which is perfectly orthorhombic, has small anisotropy energy and a reasonably large exchange energy compared to the resonant magnetic fields. In the case of monoclinic $CoCl_2 \cdot 6H_2O$, the anisotropy is very large, and the Nagamiya-Yosida theory did not provide a sufficiently good framework in which to interpret the experimental resonances. Date[17] constructed a theory in which the restriction of small anisotropy energy in comparison to the exchange energy was not present, but the Zeeman energy was still required to be small compared with the exchange energy. This theory worked well for $CoCl_2 \cdot 6H_2O$. In the case of $MnCl_2 \cdot 4H_2O$, it has already been mentioned that the anisotropy energy is much larger

---

[17] M. Date, J. Phys. Soc. Japan 16, 1337 (1961).

than in the case of $CuCl_2 \cdot 2H_2O$, but still not large in comparison to the exchange energy. Thus, Date's theory offers no special advantage over the Nagamiya-Yosida theory for $MnCl_2 \cdot 4H_2O$. Both theories, however, are deficient, since microwave resonances occur at magnetic-field values which are comparable to the low exchange field in $MnCl_2 \cdot 4H_2O$ ($\sim 12\,000$ Oe at $1°K$). The only theory which is valid for large external fields is that of Gorter and Haantjes,[16] but its applicability is limited to the case of $T=0°K$. Thus, there exists no theory at present which is suitable for all of our experimental observations in $MnCl_2 \cdot 4H_2O$.

The expectation that the Nagamiya-Yosida theory should be approximately valid in $MnCl_2 \cdot 4H_2O$ for low-field resonances and should become increasingly poor at higher values of the external field was borne out.

An unexpected deviation from the theory in a region where it should be valid, however, occurred at very low temperatures. A low-field b-axis resonance, which conformed very well to the theory in the temperature region of 0.6 to $1.6°K$ began to exhibit a marked deviation from the theory below $0.6°K$. In addition a new resonance appeared in this low-temperature region which exhibited properties similar to the critical-field resonance as regards linewidth, temperature dependence, and resonance behavior upon rotation of H_0 into the ac and bc planes. We do not have an explanation of these deviations but the possibility of a change in magnetic structure such as the formation of additional sublattices ought not to be excluded. Low-temperature neutron diffraction studies would be highly desirable to complement this study.

Stability of Crystals of Rare-Gas Atoms and Alkali Halides in Terms of Three-Body Interactions. II. Alkali-Halide Crystals*

Erminio Lombardi† and Laurens Jansen

International Division, Battelle Memorial Institute, Geneva, Switzerland

(Received 22 June 1964)

By extending the theory developed in a previous publication for the stability of rare-gas crystals, it is shown that the stability of alkali-halide crystals can be explained in terms of three-body exchange interactions between the ions. As in the case of rare-gas crystals, the analysis is based on a first- and second-order perturbation calculation with a Gaussian effective-electron model. The different size of anion and cation of each solid is taken into account. The effect on stability of double-exchange contributions to the three-body energy (negligible for rare-gas crystals) is analyzed in detail. It is shown that the theory accounts for all observed regularities on a quantitative basis. In particular, cesium chloride, bromide, and iodide are found to be stable in the cesium chloride modification; furthermore, calculated and observed values for the pressure of transition from the sodium chloride to the cesium chloride configuration are in good agreement.

INTRODUCTION

ACCORDING to the Born-Mayer theory of ionic crystals, all alkali halides should crystallize at normal pressures and temperatures in the sodium chloride structure (two interpenetrating face-centered cubic lattices), this configuration being favored over the cesium chloride structure (two interpenetrating simple-cubic lattices) by as much as a few kcal/mole. However, all cesium halides, except its fluoride, show the cesium chloride modification, whereas all rubidium and potassium halides, except potassium fluoride, have been found to exhibit pressure transitions from the sodium chloride to the cesium chloride structure. Such transitions are indeed predicted by the Born-Mayer theory, but the calculated transition pressures for the heavier alkali halides are considerably higher than those observed. For example, rubidium chloride has an experimental transition pressure of 4900 atm, whereas the calculated value is 39 000 atm.

This stability problem has received extensive attention in the literature; for detailed reviews we refer to the excellent treatises by Born and Huang[1] and by Pauling.[2] Historically, the first analysis was carried out by Hund[3] on the basis of a pair potential between the ions consisting of electrostatic interactions between point charges and a repulsive potential varying as the inverse nth power with distance. It was found that the cesium chloride modification is only stable for values of n higher than 30, but such high values are incompatible with experimental results on compressibilities of the

---

[1] M. Born and K. Huang, *Dynamical Theory of Crystal Lattices* (Oxford University Press, New York, 1954), Chaps. I and III.

[2] L. Pauling, *The Nature of the Chemical Bond* (Cornell University Press, Ithaca, New York, 1948), Chap. X.

[3] F. Hund, Z. Physik 34, 833 (1925).